Fuel 429 (2027) 140736

Contents lists available at ScienceDirect

Fuel

journal homepage: www.elsevier.com/locate/fuel

Full Length Article

Hydrogen carrier with ring dehydrogenation and lactonization in the same molecule: A thermodynamic perspective

Karsten Müller [a,b], Peter Wasserscheid [c,d,e], Sergey P. Verevkin [a,b,*]

[a] Institute of Technical Thermodynamics, University of Rostock 18059 Rostock, Germany
[b] Competence Centre °CALOR at the Department Life, Light & Matter of the Faculty of Interdisciplinary Research, University of Rostock 18059 Rostock, Germany
[c] Institute of Chemical Reaction Engineering, Friedrich-Alexander-Universität Erlangen-Nürnberg, Egerlandstr. 3, 91058 Erlangen, Germany
[d] Forschungszentrum Jülich, Institute for a Sustainable Hydrogen Economy, An der Deutschen Welle 7a, 52428 Jülich, Germany
[e] Forschungszentrum Jülich, Helmholtz-Institute Erlangen-Nürnberg for Renewable Energy (IET-2), Cauerstraße 1, 91058 Erlangen, Germany

ARTICLE INFO

Keywords:
Hydrogen storage, LOHC
Enthalpies of phase transitions
Enthalpy of formation
Vapour pressure
Quantum-chemical calculations
Reaction thermodynamics

ABSTRACT

Organic hydrogen carrier molecules can operate based on different chemical principles. A rather conventional approach is the reversible hydrogenation of an aromatic ring. A more recent alternative, with promising thermodynamic characteristics, is the lactonization of diols. These lactone systems can release hydrogen at much lower temperatures, while at the same time requiring more effort for hydrogen uptake. In this work, the combination of both reaction mechanisms within one molecule is evaluated from a thermodynamic point of view. For this task, calorimetric measurements have been applied and validated with quantum-chemical calculations to assess enthalpies and entropies of reaction. These data form the basis for a subsequent calculation of the composition of the reaction mixture as a function of pressure. The results show that dehydrogenation will proceed stepwise. Hydrogen release can start under mild conditions through lactonization (releasing up to 40% of the overall stored H_2) and, after the carrier is further heated, full hydrogen release can proceed via aromatization.

1. Introduction

Liquid Organic Hydrogen Carrier (LOHC) are a very promising approach for the storage of hydrogen in a safe and dense form. LOHC systems store hydrogen by a chemical reaction that consumes hydrogen and can be reversed recovering the original carrier, which has a preferably liquid state under ambient conditions. To achieve this, different types of reaction can be utilized. The most established class of reactions is the hydrogenation of aromatic components [1]. A major advantage of aromatic hydrogenation is the comparatively easy hydrogen uptake enabling hydrogen uptake at pressures below 10 bar [2]. However, because of the high thermodynamic driving force for hydrogen uptake, hydrogen release is more demanding. The corresponding hydrogen-rich form is an alicyclic substance that can be dehydrogenated at much milder conditions than aliphatic compounds. Nevertheless, temperature of about 553 K are still needed for the dehydrogenation of homocyclic LOHCs like methylcyclohexane [3], which necessitates heat supply at a comparatively high temperature level. Somewhat lower temperatures would be sufficient for nitrogen containing aromatic heterocycles like N-ethyl-carbazole [4] or methyl-indole [5]. However, these carriers are subject to challenging decomposition behaviour and in some cases unfavourable solid–liquid equilibria [6].

An alternative class of LOHC systems is based on lactone/diol pairs. Herein, hydrogen provision is realized by the lactonization of diols under the release of two hydrogen molecules [7]. This reaction can be realized under comparatively low temperatures [8]. The reverse step, the hydrogenation of the lactone to the diol has a rather low thermodynamic driving force, which leads to an enhanced effort for hydrogenation. The idea of this work is to combine both reactions in one molecule as shown in Fig. 1. To the best of our knowledge, this approach has not been published so far.

Indeed, the phthalide molecule (**D**) can take up to five hydrogen molecules through hydrogenation of its aromatic ring (reaction **R2**) and by opening the lactone ring (reaction **R1**). The resulting hydrogen-rich counterpart, 1,2-bis-(hydroxymethyl)cyclohexane provides a gravimetric hydrogen capacity of 6.93% and a volumetric storage capacity of 2318 Wh/L. Despite these very attractive values, an evaluation of a potential technical use of such LOHC system must consider the melting

* Corresponding author at: Institute of Technical Thermodynamics, University of Rostock, 18059 Rostock, Germany.
E-mail address: sergey.verevkin@uni-rostock.de (S.P. Verevkin).

https://doi.org/10.1016/j.fuel.2026.140736
Received 6 June 2026; Received in revised form 7 July 2026; Accepted 18 July 2026
Available online 24 July 2026

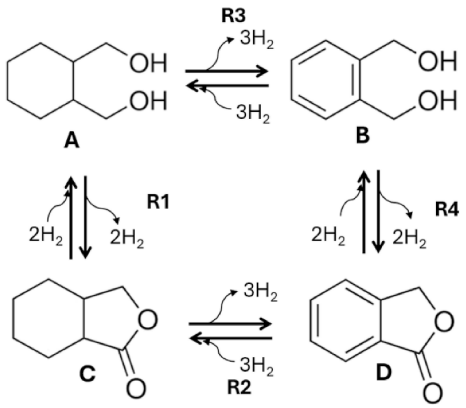

Fig. 1. The phthalide/1,2-bis-(hydroxymethyl)cyclohexane LOHC system: hydrogen release involves a reaction cascade involving lactonization of the diol function (R1, R4) and aromatization (R2, R3). 1,2-bis-(hydroxymethyl)cyclohexane (**A**) can either convert to 1,2-bis-(hydroxymethyl)benzene (**B**) or 6H-phthalide (**C**) followed by phthalide (**D**) formation.

points of the individual LOHC components which are, *e.g.* 43–45 °C for 1,2-bis-(hydroxymethyl)cyclohexane and 71–73 °C for phthalide. Thus, for practical LOHC applications, of another LOHC system might be required to inhibit crystal formation, which leads to lower melting points. In this paper, however, we focus on the thermodynamic aspects of hydrogen storage in a molecular system that combine two distinct chemical mechanisms for hydrogenation and dehydrogenation within a single compound. The fact that the thermodynamic driving forces of the two reaction steps are very different raises the question of how this difference affects the chemical properties of the process. Because of different thermodynamic properties of the two reactions, different temperatures might be needed for hydrogen release. The reaction that could be carried out under milder conditions can also be done at higher temperatures. However, this comes with some disadvantages. For instance, benefits with regards to thermal integration cannot be fully utilized. Furthermore, stability might become an issue if functional groups are in contact with catalytically active material at temperatures much higher than needed for their desired reaction.

The thermodynamic driving force of a chemical reaction is determined by the Gibbs reaction energy, $\Delta_r G^o_m$. According to the Gibbs–Helmholtz equation, it consists of both, an energetic and entropic contribution:

$$\Delta_r G^o_m = \Delta_r H^o_m - T \times \Delta_r S^o_m \quad (1)$$

where $\Delta_r H^o_m$ is the standard molar reaction enthalpy and $\Delta_r S^o_m$ is the standard entropy change of the chemical reaction. As a rule, the $\Delta_r H^o_m$-values are calculated from the standard molar enthalpies of formation, $\Delta_f H^o_m$, of reactants according to the Hesśs Law and $\Delta_r S^o_m$, are calculated from the absolute entropies, S^o_m, of the reactants. In the last century, the majority of these values were derived from experiments. In the last two decades, however, highly accurate quantum chemical calculations have played an increasingly important role in process engineering, serving to supplement and validate time-consuming experimental methods [9].

In this study, a combination of quantum chemical, experimental and empirical methods has been utilized to gain insights into the thermochemistry for the phthalide/1,2-bis-(hydroxymethyl)cyclohexane LOHC system, in which ring dehydrogenation and lactonisation occur within the same molecule. The workflow of the thermochemical steps leading to the equilibrium constants and product distribution in the system as shown in Fig. 1 was established in our previous work [10]. The key details are outlined in the electronic supplementary information (ESI).

2. Theoretical and experimental methods

Quantum chemical calculations were carried out using the Gaussian 16 program suite [11]. For each molecule presented in Fig. 1, lowest-energy conformers were identified with the CREST (conformer–rotamer ensemble sampling tool) approach (see details in ESI), and their H_{298} values were computed at the G4 [12] level of theory within the rigid-rotator harmonic-oscillator approximation. These values were subsequently converted into standard molar enthalpies of formation in the gas phase, $\Delta_f H^o_m$(g, 298 K)$_{QC}$, and analyzed accordingly. The S^o_m(g, 298 K)$_{QC}$ values were calculated according to (Eq. (1)) using H_{298} and G_{298} from the output file. The general details of the calculation procedure have been published elsewhere [13].

Absolute vapor pressures of liquid sample of 1,2-bis-(hydroxymethyl)benzene (see origin and purity in Table S1) have been measured applying the transpiration method [14,15]. Subsequently, and the standard molar enthalpy of vaporisation, $\Delta^g_l H^o_m$(298 K), and the standard molar entropy of vaporisation, $\Delta^g_l S^o_m$(298 K), could be calculated from their temperature dependence based on the Clausius-Clapeyron equation. The boiling points at reduced pressures of substances **A**–**D** were retrieved from literature and were also utilized to derive the enthalpies and entropies of vaporisation. A brief overview of the methodology and relevant experimental and computational details are provided in the ESI.

3. Results and discussion

3.1. Step I: Gas-phase enthalpies of formation and entropies from quantum-chemical calculations

Careful conformational analysis and the selection of the most stable conformers are among the most challenging tasks in quality control calculations, particularly for molecules as flexible as 1,2-bis-(hydroxymethyl)cyclohexane (**A**) and 1,2-bis-(hydroxymethyl)benzene (**B**), which may also be prone to forming intramolecular hydrogen bonds.

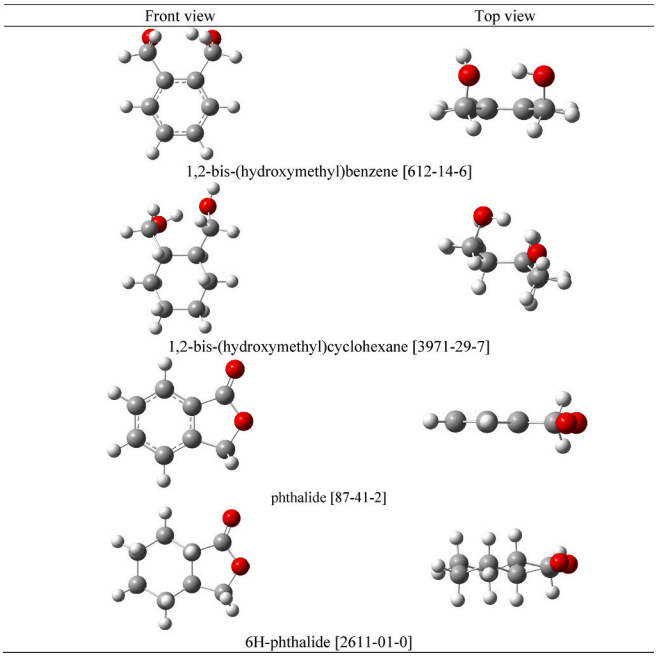

Fig. 2. Structures of the most stable conformers of the aromatic and aliphatic diols, and lactones from Fig. 1. In fact, the most stable conformations of both aromatic and aliphatic diols exhibit structures in which the distances between hydrogen and oxygen meet the criteria for intramolecular hydrogen bonding [16].

The most stable conformers of the diols and lactones are shown in Fig. 2.

The general algorithm of quantum-chemical calculations provides in the final output file the total energies E_0 at zero Kelvin, the total enthalpies at 298 K (H_{298}) and Gibbs free energies (G_{298}). In this work, the atomisation (AT) reaction formed the basis for deriving the thermochemical quantities involved in Eq. (1). The atomization approach is commonly used to determine the standard enthalpy of formation from quantum-chemical calculations. First, the atomization enthalpy is obtained by calculating the energy required to dissociate a molecule into its constituent gas-phase atoms. The standard enthalpy of formation is then derived using Hess's law by combining the calculated atomization enthalpy with the experimentally known standard enthalpies of formation of the isolated atoms. This method takes advantage of the high accuracy of quantum-chemical calculations for relative energies while anchoring the results to the experimental thermochemical scale through atomic reference data. As an example, the atomisation reaction for 1,2-bis-(hydroxymethyl)cyclohexane (**A**) can be written as follows:

$$C_8H_{16}O_2 \rightarrow 8 \times C + 16 \times H + 2 \times O \quad (2)$$

From our experience, the AT reaction is less biased and less affected by the data quality of thermochemical data in comparison to the isodesmic, isogyric, *etc.* reactions, since the reference data for the elements are known with high accuracy [17]. However, atomisation-based results regarding the enthalpy of formation, $\Delta_f H^o_m(g)$, need to be calibrated using a set of structurally related compounds for which reliable experimental enthalpies of formation $\Delta_f H^o_m(g)_{exp}$ are available [13]. As a rule, there is a simple linear relationship between the AT results and the experimental data, and the parameters of this linear correlation are used to "correct" the AT results. The $\Delta_f H^o_m(g)_{AT}$ results from the G4 calculations (see Table 1, column 3) and the corresponding "corrected" $\Delta_f H^o_m(g)_{QC}$-values (see Table 1, column 4) are summarised in Table 1.

The results of the G4 calculations of the absolute entropies of diols and lactones in the ***gas phase***, shown in Table 1, column 4, were corrected for the contribution of conformational entropy [18], as outlined in the ESI; the corrected values are shown in Table 1, column 6. Thus, both the enthalpy and entropy contributions to Eq. (1) were obtained via the G4 quantum chemical method. However, as the storage and release of hydrogen in diol/lactone LOHC systems can effectively take place in the liquid phase, the corresponding ***liquid-phase*** values $\Delta_f H^o_m(liq)$ and $S^o_m(liq)$ of the reactants shown in Fig. 1 are very useful as well. The conversion of the quantum chemical results for the gas phase to the liquid phase can be achieved via the general thermodynamic relationships:

$$\Delta_f H^o_m(liq, 298K) = \Delta_f H^o_m(g, 298K)QC - \Delta^g_l H^o_m(298K) \quad (3)$$

$$S^o_m(liq, 298K) = S^o_m(g, 298K) - \Delta^g_l S^o_m(298K) \quad (4)$$

The values for enthalpy $\Delta^g_l H^o_m$(298 K) and entropy $\Delta^g_l S^o_m$(298 K) of vaporization have been derived as described in the following section.

3.2. Step II: Evaluation of the liquid–gas phase transition thermodynamics

The absolute vapor pressures of the LOHC hydrogen-lean and hydrogen-rich counterparts are important thermodynamic parameters for the thermochemical evaluation of chemical reactions and for development of hydrogen storage technologies. It is expected that these will not be too high, to ensure high hydrogen purities and to mitigate safety risks. Moreover, the temperature dependencies of vapour pressure provide a practical method for deriving the thermodynamics of vaporisation (enthalpy and entropy over a wide temperature range), including the $\Delta^g_l H^o_m$(298 K) and $\Delta^g_l S^o_m$(298 K) values, which are commonly adjusted to the reference temperature $T = 298$ K and are listed in tabular form in databases and reference compilations [19]. The data available in the literature on the vapour pressures of molecules **A**–**D** are very limited (see Table S7). For 1,2-bis(hydroxymethyl)benzene (**B**), only three experimental measurements in the range of 413 to 603 K were found in the literature (see Table S7). As the enthalpy of vaporisation of **B** derived from these few data points could be of questionable reliability, complementary vapour pressure measurements for this compound were carried out in this study (see Table S6) over a temperature range (340.2 K – 372.1 K) as close as possible to the reference temperature $T = 298$ K. Details, as well as the equations used to approximate the temperature dependence of vapour pressures and to determine the thermodynamic vaporisation parameters, are outlined in the ESI. The results for the vaporisation enthalpies, $\Delta^g_l H^o_m$(298 K), and entropies, $\Delta^g_l S^o_m$(298 K), are summarised in Table 2.

It strikes that the accurate transpiration result $\Delta^g_l H^o_m(298\ K) = 91.2 \pm 0.7$ kJ·mol^{-1} for (**B**) agrees well with the estimate $\Delta^g_l H^o_m(298\ K) = 92.0 \pm 4.3$ kJ·mol^{-1}, which is based on three data points near the normal boiling point. This agreement could be regarded as good evidence for the method of adjusting the enthalpies of vaporization to the reference temperature $T = 298$ K (see ESI for further details). In view of this optimistic conclusion, the enthalpy of vaporisation $\Delta^g_l H^o_m(298\ K) = 96.0 \pm 3.8$ kJ·mol^{-1} (see Table 2), for 1,2-bis-(hydroxymethyl)cyclohexane (**A**), which was derived from the approximation of boiling points at reduced pressure, is likely to be reliable. However, to justify this optimism, the enthalpy of vaporisation of (**A**) was additionally assessed from the structure–property relationships shown in Fig. 3.

It is quite obvious from Fig. 3 that the structure of 1,2-bis-(hydroxymethyl)cyclohexane (**A**) looks as though 1,4-butanediol has fused with cyclohexane. The enthalpies of vaporisation for these two simple molecules are well known [10,22], therefore, the transformation of the "centerpiece" molecule 1,4-butanediol using building blocks or increments (derived from cyclohexane, see Table S10) enables the construction of (**A**) with the numerical value $\Delta^g_l H^o_m(298\ K) = 95.6 \pm 2.0$

Table 1
Results of the G4 calculations of the gas-phase enthalpies of formation and entropies of diols and lactones at $T = 298$ K (in kJ·mol^{-1}).

CAS	Compounds	$\Delta_f H^o_m(g)_{AT}$ [a]	$\Delta_f H^o_m(g)_{QC}$ [b]	$S^o_m(g)$ [c]	$S^o_m(g)_{corr}$ [d]
		kJ·mol^{-1}	kJ·mol^{-1}	J·mol^{-1}·K^{-1}	J·mol^{-1}·K^{-1}
1	2	3	4	5	6
3971-29-7	1,2-bis-(hydroxymethyl)-cyclohexane (**A**)	−490.4	−490.0 [Table S3]	411.5	428.2
612-14-6	1,2-bis-(hydroxymethyl)-benzene (**B**)	−285.6	−285.9 [Table S2]	387.6	404.2
2611-01-0	6H-phthalide (**C**)	−419.1	−415.9 [Table S5]	372.1	372.1
87-41-2	phthalide (**D**)	−229.4	−221.3[Table S4]	351.8	351.8

[a] Calculated using the G4 method according to the atomisation (AT) reaction.
[b] Atomisation results were corrected with help of reliable experimental literature data using the corresponding equations developed in Tables S2–S5: Uncertainties are assessed to be ±3.5 kJ·mol^{-1} (0.95 level of confidence with k = 2) [12].
[c] Calculated using the G4 method.
[d] Corrected with the number of rotatable bonds (further details are provided in ESI).

Table 2
Summary of standard molar enthalpies and entropies of vaporisation of diols and lactones.

CAS	Compound	M [a]	T-range	$\Delta_l^g H_m^o(T_{av})$ [b]	$\Delta_l^g H_m^o$(298 K) [c]	$\Delta_l^g S_m^o$(298 K) [d]	Ref.
			K	kJ·mol^{-1}	kJ·mol^{-1}	J·mol^{-1}·K^{-1}	
3971–29-7	(**A**)	BP	393–543	77.7 ± 0.9	96.0 ± 3.8	193.0 ± 3.1	Table S7
		CP			95.6 ± 2.0		Fig. S2
					95.7 ± 1.8 [c]		
612–14-6	(**B**)	T	340.2–372.1	83.4 ± 0.5	91.2 ± 0.7	174.7 ± 2.0	Table S6
		BP	413–603	71.5 ± 1.3	92.0 ± 4.3		
					91.2 ± 0.8 [c]		
2611–01-0	(**C**)	BP	337–503	72.3 ± 0.8	77.6 ± 1.3	162.5 ± 2.9	20
87–41-2	(**D**)				74.7 ± 0.8	144.5 ± 2.6	20

[e] Weighted mean value (uncertainties were taken as the weighting factor). Values given in bold are recommended for further thermochemical calculations.
[a] Methods: T = transpiration method; BP = estimated from boiling points at different pressures (see Table S7) CP = calculated using the "centerpiece" (CP) approach with 1,4-pentanediol as the "centerpiece" molecule (see Figs. S2).
[b] Vapour pressures available in the literature were treated using Eqs. (S10) – (S15) with help of heat capacity differences from Table S8 to calculate the enthalpies of vaporisation at 298 K. Uncertainties of the sublimation/vaporisation enthalpies $U(\Delta_l^g H_m^o)$ are the expanded uncertainties (0.95 level of confidence). They include uncertainties from the fitting equation and uncertainties from temperature adjustment to $T = 298$ K. Uncertainties in the temperature adjustment of vaporisation enthalpies to the reference temperature $T = 298$ K are estimated to account with 20% to the total adjustment.
[c] Standard molar enthalpy of vaporisation, calculated according to Eq. (S11).
[d] Standard molar entropy of vaporisation, calculated according to Eq. (S16).

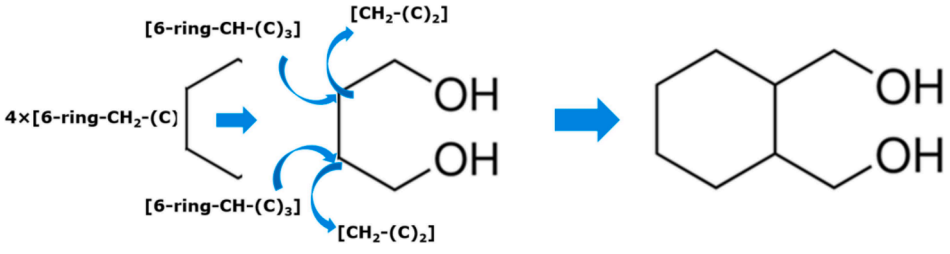

Fig. 3. Calculating the enthalpy of vaporization, $\Delta_l^g H_m^o$(298 K)/kJ·mol^{-1} of 1,2-bis-(hydroxymethyl)cyclohexane (A) using the "centerpiece approach" [21] and the 1,4-butanediol $\Delta_l^g H_m^o$(298K)=79.1 ± 0.5 kJ·mol^{-1} [10]), as the staring molecules. The numerical values of required for calculations increments are given in Table S10.

kJ·mol^{-1}, which is indistinguishable from the BP estimate of $\Delta_l^g H_m^o$(298 K) = 96.0 ± 3.8 kJ·mol^{-1} (see Table 2). This agreement not only enhances the reliability of the results evaluated for (**A**), but also emphasises the significance of empirical structure–property methods for the cross-validation of experimental data. Since the vaporisation enthalpies of 6H-phthalide (**C**) and phthalide (**D**) were only recently evaluated (see Table 2), in our study [20], a cross-validated set of reliable vaporisation enthalpies, $\Delta_l^g H_m^o$(298 K), for molecules **A**–**D** from Table 2 is now ready for use in the third step.

3.3. Step III: From thermodynamics in the gas phase to the liquid phase

The gas-phase enthalpies of formation, $\Delta_f H_m^o$(g, 298 K)$_{QC}$, and absolute entropies in the gas-phase, S_m^o(g, 298 K)$_{QC}$, derived from QC-calculations (see Table 1) can be now combined with the validated vaporisation enthalpies $\Delta_l^g H_m^o$(298 K) and vaporisation entropies $\Delta_l^g S_m^o$(298 K) (see Table 2) to drive the liquid phase enthalpies of formation, $\Delta_f H_m^o$(liq, 298 K)$_{theor}$ and the liquid-phase absolute entropies, S_m^o(liq, 298 K)$_{theor}$ according to Eqs. (3) and (4) for reactants shown in Fig. 1. These results are summarized in Tables 3 and 4.

The enthalpy and entropy values derived in Tables 3 and 4 are now sufficient to serve as input into the Gibbs-Helmholtz equation, Eq. (1), so that the final general thermodynamic analysis of the reactant conversion shown in Fig. 1 can be carried out, as follows.

Table 3
Calculation of the liquid-phase enthalpies of formation, $\Delta_f H_m^o$(liq)$_{theor}$, for diols and lactones from the quantum-chemical enthalpies of formation, $\Delta_f H_m^o$(g)$_{QC}$, and the standard molar enthalpies of vaporisation, $\Delta_l^g H_m^o$, of diols and lactones (at $T = 298$ K and $p^\circ = 0.1$ MPa, in kJ·mol^{-1}).

Compound	$\Delta_f H_m^o$(g)$_{QC}$ [a]	$\Delta_l^g H_m^o$ [b]	$\Delta_f H_m^o$(liq)$_{theor}$ [c]
1,2-bis-(hydroxymethyl)-cyclohexane (**A**)	−490.0	95.7 ± 1.8	−585.7
1,2-bis-(hydroxymethyl)-benzene (**B**)	−285.9	91.2 ± 0.8	−377.1
6H-phthalide (**C**)	−415.9	77.6 ± 1.3	−493.5
phthalide (**D**)	−221.3	74.7 ± 0,8	−296.0

[a] From Table 1.
[b] From Table 2.
[c] Difference between column 2 and 3 in this table.

3.4. Step IV: General thermodynamic analysis of the reaction cascade

3.4.1. Reaction enthalpies, entropies and Gibbs free energies

The theoretical values $\Delta_f H_m^o$(298 K) and S_m^o(298 K) determined in Tables 3 and 4 were used to calculate the reaction enthalpies, $\Delta_r H_m^o$(298 K), and entropies, $\Delta_r S_m^o$(298 K), of the lactonisation reactions **R1** and **R4**, as well as the hydrogenation reactions **R2** and **R3**, in both the gaseous and liquid phases (see Table 5).

The latter values were used to calculate the gas-phase and liquid phase **total** Gibbs free reaction energies, $\Delta_r G_m^o$(g or liq, T) at three practically relevant temperatures 298 K, 400 K and 500 K (see Table 6).

Table 4
Calculation of the liquid-phase entropies, $S^{o}_{m}(liq)_{theor}$, for diols and lactones from the absolute standard molar entropies, $S^{o}_{m}(g)$, and the standard molar entropies of vaporisation, $\Delta^{g}_{l}S^{o}_{m}$, of diols and lactones (at $T = 298$ K and $p^{\circ} = 0.1$ MPa, in J·mol^{-1}·K^{-1}).

Compound	$S^{o}_{m}(g)$ [a]	$\Delta^{g}_{l}S^{o}_{m}$ [b]	$S^{o}_{m}(liq)_{theor}$ [c]	$C^{o}_{p,m}(g)$ [d]
1,2-bis-(hydroxymethyl)-cyclohexane (**A**)	428.2	193.0 ± 3.1	235.2	175.9
1,2-bis-(hydroxymethyl)-benzene (**B**)	404.2	174.7 ± 2.0	229.5	154.4
6H-phthalide (**C**)	372.1	162.5 ± 2.9	209.6	146.3
phthalide (**D**)	351.8	144.5 ± 2.6	207.3	125.3

[a] Corrected values from Table 1, column 6.
[b] From Table 2.
[c] Difference between column 2 and 3 in this table.
[d] Calculated using B3LYP/6–31 g(d,p).

The $\Delta_{r}G^{o}_{m}$(g or liq, T)-values derived according to Eq. (1) allow the modeling of the products distribution in equilibrium for the LOHC system shown in Fig. 1.

3.4.2. Reaction equilibrium

The reaction equilibrium determines the maximum extent of reaction that can be reached at given conditions. The composition in equilibrium is the same if the reaction is performed as dehydrogenation of 1,2-bis-(hydroxymethyl)cyclohexane (**A**) or hydrogenation of **D** (phthalide), respectively. Based on the data for enthalpy and entropy as well as the vapor pressure data (because the reaction happens in a biphasic system) it is possible to calculated this equilibrium. In this work, the equilibrium modeling was carried out by first calculating equilibrium constant from the enthalpy and entropy values measured in this work and converting them to reaction temperature utilizing the vant-Hoff equation. In a second step, the system of two equations (for the reaction-extent and for the superimposed vapor–liquid equilibrium) is solved to calculate the share of the different compounds in the two phases in equilibrium. The calculation of reaction equilibria, also in systems with different competing equilibria is described elsewhere [23]. Generally, two types of non-ideality have to be included in such calculations: non-ideality of the liquid mixture (activity coefficients) and, at least at elevated pressures, deviation from ideal gas behaviour (fugacity coefficients). Yet, as sensitiviy of the resulting equilibrium curves is rather low, these effects have only negligibly effects under the conditions studied.

Fig. 4 shows the share of the four species in equilibrium as a function of pressure at a given temperature of 500 K. At very high pressures of 40 bar and higher the completely hydrogenated species **A** (1,2-bis-(hydroxymethyl)cyclohexane) would dominate the reaction system.

Table 6
The gas-phase and liquid phase **total** Gibbs free reaction energies, $\Delta_{r}G^{o}_{m}$, (at $p^{\circ} = 0.1$ MPa in kJ·mol^{-1}) for reactions **R1** to **R4**, calculated according to the Gibbs-Helmholtz equation.

		$\Delta_{r}G^{o}_{m}$ [a] (298 K)	$\Delta_{r}G^{o}_{m}$ [b] (400 K)	$\Delta_{r}G^{o}_{m}$ [b] (500 K)
R1	gas	12.9	−8.4	−30.2
	liq	21.9	−2.1	−25.8
R4	gas	2.3	−19.4	−41.5
	liq	9.8	−14.6	−38.6
R2	gas	83.8	45.0	4.9
	liq	81.3	40.7	−1.3
R3	gas	94.4	56.0	16.3
	liq	93.4	53.1	11.5

[a] Calculated according to Eq. (1).
[b] The $\Delta_{r}G^{o}_{m}$(298 K)-values from column 3 were adjusted to 400 K and 500 K as shown in ESI.

This means that either the extent of dehydrogenation would be negligible or, if it is a hydrogenation of the dehydrogenated form, hydrogenation can nearly reach completion if sufficient time is given to the reaction system in presence of a suitable hydrogenation catalyst. However, at moderate pressures a significant amount of **C** (6H-phthalide) is formed by partial dehydrogenation through lactonization, while the formation of **B** (1,2-bis-(hydroxymethyl)benzene) and **D** (phthalide), which both require dehydrogenation of the cyclohexyl ring, remains below 1% at ambient pressure or higher.

The very small amounts of the two species with an aromatic ring (**B** and **D**) is due to the low thermodynamic driving force for the

Table 5
Calculation of the reaction enthalpies, $\Delta_{r}H^{o}_{m}$, and entropies, $\Delta_{r}S^{o}_{m}$, of lactonisation reactions **R1** and **R4 (Diol → Lactone)** and hydrogenation reactions **R2** and **R3** (**Ar → 6H-Ar**) in the gaseous and liquid phases (in kJ·mol^{-1} or J·mol^{-1}·K^{-1} at $T = 298$ K and $p^{\circ} = 0.1$ MPa).

		$\Delta_{f}H^{o}_{m}$ [a]	$\Delta_{f}H^{o}_{m}$ [a]	$\Delta_{r}H^{o}_{m}$ [b]	$\Delta_{r}H^{o}_{m}/H_2$ [c]	S^{o}_{m} [d]	S^{o}_{m} [d]	$\Delta_{r}S^{o}_{m}$ [e]	$\Delta_{r}S^{o}_{m}/H_2$ [f]
1	2	3	4	5	6	7	8	9	10
		Diol	**Lactone**			**Diol**	**Lactone**		
R1	gas	−490.0	−415.9	74.1	37.1	372.1	372.1	205.3	102.6
	liq	−585.7	−493.5	92.2	46.1	209.6	209.6	235.8	117.9
R4	gas	−285.9	−221.3	64.6	32.3	404.2	351.8	209.0	104.5
	liq	−377.1	−296.0	81.1	40.6	229.5	207.3	239.2	119.6
		Ar	**6H-Ar**			**Ar**	**6H-Ar**		
R2	gas	−221.3	−415.9	194.6	64.6	351.8	372.1	371.7	123.9
	liq	−296.0	−493.5	197.5	65.8	207.3	209.6	389.7	129.9
R3	gas	−285.9	−490.0	204.1	68.0	404.2	428.2	368.0	122.7
	liq	−377.1	−585.7	208.6	69.5	229.5	235.2	383.6	128.8

[a] From Table 3, column 4.
[b] Reaction enthalpies calculated using Hess's law and the entries in columns 3 and 4.
[c] Reaction enthalpies related to 1 mol of hydrogen released (in kJ·mol^{-1}–H_2).
[d] From Table 4, column 4.
[e] Reaction entropies calculated using the entries in columns 7 and 8.
[f] Reaction entropies related to 1 mol of hydrogen released (in J·mol^{-1}·K^{-1}–H_2).

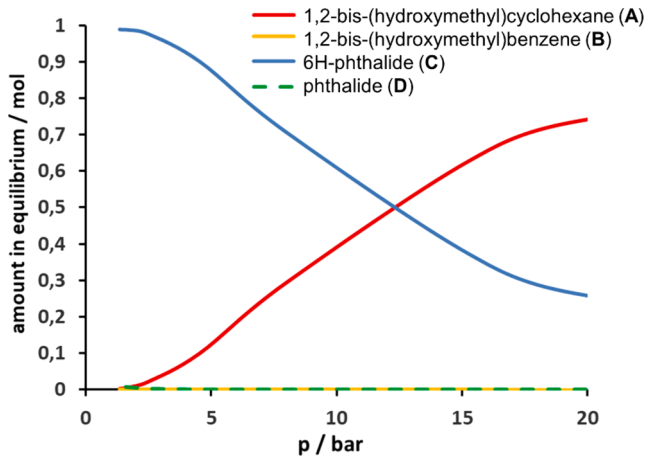

Fig. 4. Reaction equilibrium as a function of pressure for the (de)hydrogenation cascade of reactions shown in Fig. 1 at 500 K.

dehydrogenation of alicyclic rings at the moderate temperature of 500 K. Hence, the lactonization reaction can take place for hydrogen release, but ring dehydrogenation remains secondary. Species **D** (phthalide) dominates over **B** (1,2-bis-(hydroxymethyl)benzene) at moderate pressures, because most of the molecules with a dehydrogenated homocyclic ring will also undergo lactonization (either first or second). Only at high pressures the shares become similar as lactonization gets unfavorable, too.

A change in temperature would cause the opposite effects as a change in pressure. If temperature would be increased equilibrium shifts towards the dehydrogenated species. This is true for both types of reactions, lactonization and ring dehydrogenation. Nevertheless, the effect of a change in temperature is more pronounced in case of the dehydrogenation/hydrogenation of the alicyclic/aromatic ring. This is due to the higher enthalpy of reaction, which is about twice as high than for lactonization (temperature dependence of equilibrium constant is determined by enhalpy of reaction through the vant-Hoff equation). Yet, within the whole temperature range technical relevant for hydrogen storage, the thermodynamic driving force for lactonization stays significantly larger than for dehydrogenation of alicyclic rings. Nevertheless, as already known from several previous works on LOHCs, these dehydrogenations become thermodynamically favorable enough to enable a technical hydrogen release process at about 550 K.

The reaction equilibrium does not allow reliable conclusions on reaction pathways. However, the thermodynamic driving forces, which govern the equilibrium, are indicators for favoured reaction paths. The thermodynamic observation clearly indicate that hydrogen release, even at high temperatures, will under most conditions first proceed via lactonization. Vice versa, hydrogen uptake is most likely to first mainly proceed through hydrogenation of the aromatic ring, while the opening of the lactone ring is rather demanding. Note, that different types of catalyst may be most suitable to catalyze the different hydrogenation and dehydrogenation steps. While Cu-based catalysts are well-known to promote the lactonization and the diol formation steps [24,25], platinum group metal-based catalysts are most suitable for the aromatics hydrogenation and alicyclics dehydrogenation step [26,27].

4. Conclusions

Hydrogen storage through two different reaction types, both combined in one carrier molecule, leads to a complicated, but interesting thermochemical situation. As the thermodynamic driving forces for dehydrogenation of alicyclic rings and lactonization of diols strongly vary, hydrogen release will proceed in a stepwise manner. First, the diol forms a lactone ring on the molecule, releasing two hydrogen molecules. Second, the alicyclic ring is dehydrogenated, releasing three hydrogen molecules. However, as long as temperature remains within a certain window ("high enough" for lactonization, but "too low" for dehydrogenation of the ring) thermodynamics prohibit significant dehydrogenation of the alicyclic part of the molecule but already enable lactonization. Thus, only about 40% of the hydrogen can be released. Nevertheless, this does not necessarily have to be a disadvantage. For instance, special reactor designs might make use of the fact that a certain share of the hydrogen release can be facilitated at lower temperatures, before the carrier is fully heated to reaction temperature for the dehydrogenation of the alicyclic ring. Such a two-zone reactor would first operate at lower temperatures with a catalyst for lactonization and afterwards at higher temperatures with a catalyst for ring dehydrogenation at higher temperatures. Heat supply to the different zones could be done at different temperature levels utilizing low grade heat for the first part. However, technically more relevant is probably the utilization as a LOHC with rather fast startup from a cold state, because lactonization could already provide hydrogen long before temperatures for ring dehydrogenation are reached.

In contrast, hydrogen uptake will first proceed via hydrogenation of the aromatic ring, while opening of the lactone ring has a rather low thermodynamic driving force. Even though thermodynamics do not determine catalytic pathways, they still provide guidelines and set immovable limitations. As a consequence, hydrogen uptake will necessitate high pressures and a catalyst system capable of enabling hydrogenative ring opening of lactones.

CRediT authorship contribution statement

Karsten Müller: Writing – review & editing, Visualization, Validation, Project administration, Methodology, Conceptualization. **Peter Wasserscheid:** Writing – review & editing, Validation, Resources, Project administration, Methodology, Conceptualization. **Sergey P. Verevkin:** Writing – original draft, Validation, Methodology, Formal analysis, Data curation, Conceptualization.

Funding

This project has been funded by the Free State of Bavaria through the project "Oxo-LOHC – Autotherme und ultratiefe Wasserstoff-Freisetzung aus LOHC-Systemen" ("Autothermal and ultra deep hydrogen release from LOHC systems", grant number: 84-6665a2/201/11).

Declaration of competing interest

The authors declare that they have no known competing financial interests or personal relationships that could have appeared to influence the work reported in this paper.

Appendix A. Supplementary data

Supplementary data to this article can be found online at https://doi.org/10.1016/j.fuel.2026.140736.

Data availability

All data are available in the text and in the electronic supporting information

References

[1] Modisha P, Bessarabov D. Aromatic liquid organic hydrogen carriers for hydrogen storage and release. Curr Opin Green Sust Chem 2023;42:100820. https://doi.org/10.1016/j.cogsc.2023.100820.
[2] Jorschick H, Preuster P, Bösmann A, Wasserscheid P. Hydrogenation of aromatic and heteroaromatic compounds – a key process for future logistics of green hydrogen using liquid organic hydrogen carrier systems. Sust Energy Fuels 2021;5:1311–46. https://doi.org/10.1039/d0se01369b.

[3] Sekine Y, Higo T. Recent trends on the dehydrogenation catalysis of Liquid Organic Hydrogen Carrier (LOHC): a review. Top Catal 2021;64:470–80. https://doi.org/10.1007/s11244-021-01452-x.
[4] Stark K, Emel'yanenko VN, Zhabina AA, Varfolomeev MA, Verevkin SP, Müller K, Arlt W. Liquid organic hydrogen carriers: thermophysical and thermochemical studies of carbazole partly and fully hydrogenated derivatives. Ind Eng Chem Res 2015;54:7953–66. https://doi.org/10.1021/acs.iecr.5b01841.
[5] Li L, Yang M, Dong Y, Mei P, Cheng H. Hydrogen storage and release from a new promising Liquid Organic Hydrogen Storage Carrier (LOHC): 2-methylindole. Int J Hydrogen Energy 2016;41:16129–34. https://doi.org/10.1016/j.ijhydene.2016.04.240.
[6] Stark K, Keil P, Schug S, Müller K, Wasserscheid P, Arlt M. Melting points of potential liquid organic hydrogen carrier systems consisting of N-alkylcarbazoles. J Chem Eng Data 2016;61:1441–8. https://doi.org/10.1021/acs.jced.5b00679.
[7] Mevawala C, Autrey T, Brooks K, Bowden M, Tran BL, Müller K. 1,4-Butanediol as a hydrogen carrier: liquid- versus gas-phase dehydrogenation. Energy Fuels 2023;37:560–6. https://doi.org/10.1021/acs.energyfuels.2c03355.
[8] Onoda M, Nagano Y, Fujita K. Iridium-catalyzed dehydrogenative lactonization of 1,4-butanediol and reversal hydrogenation: new hydrogen storage system using cheap organic resources. Int J Hydrogen Energy 2019;44:28514–20. https://doi.org/10.1016/j.ijhydene.2019.03.219.
[9] Pracht P, Grimme S. Calculation of absolute molecular entropies and heat capacities made simple. Chem Sci 2021;12:6551–68. https://doi.org/10.1039/d1sc00621e.
[10] Siewert R, Samarov AA, Elbakari AV, Vostrikov SV, Richter M, Müller K, et al. Thermodynamics of reversible hydrogen storage with LOHC: a real game changer with diol/lactone pairs. Fuel 2027;427(Part B):139672. https://doi.org/10.1016/j.fuel.2026.139672.
[11] Frisch MJ, Trucks GW, Schlegel HB, Scuseria GE, Robb MA, Cheeseman JR, et al. Gaussian 16, Revision C.01 Gaussian, Inc., Wallingford CT; 2016.
[12] Curtiss LA, Redfern PC, Raghavachari K. Gaussian-4 theory. J Chem Phys 2007;126:084108. https://doi.org/10.1063/1.2436888.
[13] Verevkin SP, Emel'yanenko VN, Notario R, Roux MV, Chickos JS, Liebman JF. Rediscovering the wheel. thermochemical analysis of energetics of the aromatic diazines. J Phys Chem Lett 2012;3:3454–9. https://doi.org/10.1021/jz301524c.
[14] Verevkin SP, Emel'yanenko VN. Transpiration method: vapor pressures and enthalpies of vaporization of some low-boiling esters. Fluid Phase Equilib 2008;266:64–75. https://doi.org/10.1016/j.fluid.2008.02.001.
[15] Verevkin SP, Sazonova AY, Emel'yanenko VN, Zaitsau DH, Varfolomeev MA, Solomonov BN, Zherikova KV. Thermochemistry of halogen-substituted methylbenzenes. J Chem Eng Data 2015;60:89–103. https://doi.org/10.1021/je500784s.
[16] Pimentel GC, McClellan AL. The hydrogen bond. San Francisco: W.H. Freeman; 1960. p. 1–475.
[17] Chase MW. NIST-JANAF Themochemical Tables, Fourth Edition. J Phys Chem Ref Data, Monogr 1998;9:1–1951.
[18] Ghahremanpour MM, van Maaren PJ, Ditz JC, Lindh R, van der Spoel D. Large-scale calculations of gas phase thermochemistry: enthalpy of formation, standard entropy, and heat capacity. J Chem Phys 2016;145:114305. https://doi.org/10.1063/1.4962627.
[19] Verevkin SP, Emel'yanenko VN, Diky V, Muzny CD, Chirico RD, Frenkel M. New group contribution approach to thermochemical properties of organic compounds: hydrocarbons and oxygen containing compounds. J Phys Chem Ref Data 2013;42:033102. https://doi.org/10.1063/1.4815957.
[20] Siewert R, Samarov AA, Vostrikov SV, Müller K, Wasserscheid P, Verevkin SP. Hydrogenation of aromatic ethers and lactones: does the oxygen functionality really improve the thermodynamics of reversible hydrogen storage in the related LOHC systems? Oxygen 2025;5:18. https://doi.org/10.3390/oxygen5030018.
[21] Verevkin SP, Andreeva IV, Zherikova KV, Pimerzin AA. Prediction of thermodynamic properties: centerpiece approach—how do we avoid confusion and get reliable results? J Therm Anal Calorim 2022;147:8525–34. https://doi.org/10.1007/s10973-021-11115-4.
[22] Majer V, Svoboda V. Enthalpies of vaporization of organic compounds: a critical review and data compilation. Oxford: Blackwell Scientific Publications; 1985. p. 1–300.
[23] Müller K, Baumgärtner A, Mokrushina L, Arlt W. Increasing the equilibrium yield of oxidative dehydrogenation with CO2 by secondary reactions. Chem Eng Technol 2014;37:1261–4. https://doi.org/10.1002/ceat.201300823.
[24] Chen Y, Kong X, Yang C, Liao Y, Gao G, Ma R, et al. A catalytic cycle that enables crude hydrogen separation, storage and transportation. Nat Energy 2025;10:971–80. https://doi.org/10.1038/s41560-025-01806-9.
[25] Wasserscheid P. Impurity-tolerant catalysis. Nat Energy 2025;10:924–5. https://doi.org/10.1038/s41560-025-01832-7.
[26] Jorschick H, Preuster P, Dürr S, Seidel A, Müller K, Bösmann A, Wasserscheid P. Hydrogen storage using a hot pressure swing reactor. Energy Environ Sci 2017;10:1652–9. https://doi.org/10.1039/C7EE00476A.
[27] Auer F, Hupfer A, Bösmann A, Szesni N, Wasserscheid P. Influence of the nanoparticle size on hydrogen release and side product formation in liquid organic hydrogen carrier systems with supported platinum catalysts. Cat Sci Technol 2020;10:6669–78. https://doi.org/10.1039/D0CY01173H.